



# 1 The contribution of diminishing river sand loads to beach 2 erosion worldwide

3 **Vincent Regard<sup>1,†,\*</sup>, Rafael Almar<sup>2,†,\*</sup>, Marcan Graffin<sup>1,2</sup>, Sébastien Carretier<sup>1</sup>,**  
4 **Edward Anthony<sup>3</sup>, Roshanka Ranasinghe<sup>4,5,,6</sup>, Pierre Maffre<sup>3,7</sup>**

5

- 6 1. GET (Universite de Toulouse/CNRS/IRD/UPS/CNES), F31400 Toulouse, France
- 7 2. LEGOS (Universite de Toulouse/CNRS/IRD/UPS), F31400 Toulouse, France
- 8 3. CEREGE (Aix Marseille Univ, CNRS, IRD, INRAE, Coll France), F13545 Aix-en-Provence, France
- 9 4. Department of Coastal and Urban Risk & Resilience, IHE Delft Institute for Water Education, 2601 DA  
10 Delft, The Netherlands
- 11 5. Harbour, Coastal and Offshore Engineering, Deltares, 2600 MH Delft, The Netherlands
- 12 6. Water Engineering and Management, Faculty of Engineering Technology, University of Twente, 7522 NB  
13 Enschede, The Netherlands
- 14 7. Department of Earth and Planetary Science, University of Berkeley, Berkeley CA 94720-4767, California,  
15 U.S.A.

16 † these authors contributed equally

17 \* corresponding authors. [Vincent.regard@get.omp.eu](mailto:Vincent.regard@get.omp.eu), [Rafael.almar@ird.fr](mailto:Rafael.almar@ird.fr)

18

19 Journal: Natural Hazards and Earth System Sciences (NHES) [https://natural-hazards-and-earth-system-](https://natural-hazards-and-earth-system-sciences.net/)  
20 [sciences.net/](https://natural-hazards-and-earth-system-sciences.net/)

21

22



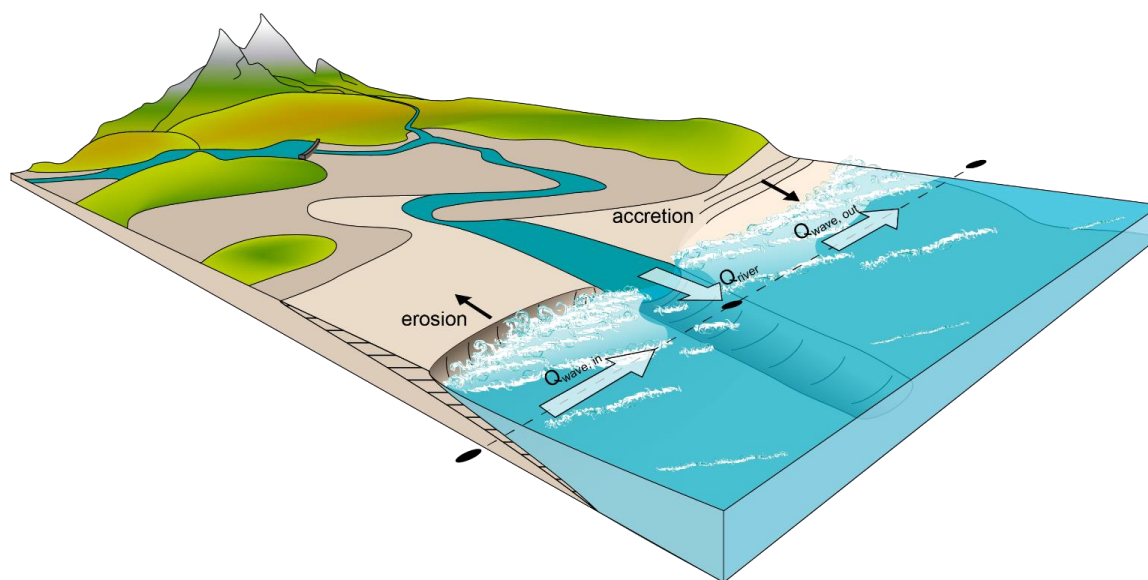
## 23 Abstract

24 The erosion of sandy beaches can have a profound impact on human activities and ecosystems, especially on  
25 developed coasts. The scientific community has, to date, primarily focused on the potential impact of changes in  
26 sea level and waves on sandy beaches. While being abundantly recognized at local to regional scales in numerous  
27 studies over the last two decades, the contribution of diminishing fluvial sediment supply to sandy beach erosion  
28 at the global scale is still to be investigated. Here, we present a model of sediment budget computed from the  
29 balance between land riverine input and coastal transport. It results in a global picture of sand pathway from land  
30 to sea. Our analysis demonstrates the massive impact of the thousands of river dams on beach erosion  
31 worldwide. Sand can be mobilized with wave-induced longshore transport over large distances, in general toward  
32 the equator, within sediment cells, often at distance from the outlets.

## 33 1 Introduction

34 Coastal zones are dynamic areas at the interface between land and sea. They concentrate a large part of the  
35 world's population (Maul and Duedall, 2019) as well as rich and rare ecosystems (Barbier et al., 2011; Dada et al.,  
36 2020). However, human activities severely affect the fragile equilibrium of these areas, notably by weakening  
37 ecological sustainability while increasing the exposure of populations to natural hazards (Oppenheimer et al.,  
38 2019). Luijendijk et al. (2018) showed, from satellite data, that about 31% of the world's ice-free coasts are  
39 fronted by sandy beaches, 24% of which are eroding at a rate exceeding 0.5 m/y. Where beach erosion prevails,  
40 social-ecological systems can be severely destabilized.

41 Sandy shoreline retreat is driven by regional and global oceanic factors such as sea-level rise and changes in wave  
42 regimes as well as local ambient processes, including fluvial sediment inputs (Vousdoukas et al. 2020; Bruun,  
43 1962; Ranasinghe, 2021; Bamunawala et al., 2020, 2021; Warwick et al., 2022, 2023). Locally, the cross-shore  
44 temporal evolution of the coastline  $\Delta X_{cross}$  can be expressed as:  $\Delta X_{cross}=f(RSLR, Waves_{cross}, \Delta Q, Q_{anthrop})$ , where  $RSLR$   
45 is the relative sea-level rise,  $Q_{anthrop}$  the amount of sediment added or removed from the beach by direct human  
46 actions (i.e., beach nourishments, sand extractions, etc...).  $Waves_{cross}$  is the equilibrium term between wave  
47 energy and cross-shore shoreline location (Yates et al., 2011; Splinter et al., 2014; Roelvink et al., 2020).  
48  $\Delta Q=Q_{river}+Q_{wave,in}-Q_{wave,out}$  is the local coastal sediment budget under natural processes (even though some of  
49 these natural processes are altered by human influences such as deep-water harbours, dikes and jetties) between  
50 sediment inputs from land  $Q_{river}$ , wave-induced longshore transport input  $Q_{wave,in}$  and loss  $Q_{wave,out}$ . A sediment  
51 imbalance in  $\Delta Q$  drives a local evolution, with a negative value signifying a sediment deficit with potential  
52 shoreline retreat and a positive value an accumulation of sediment with shoreline progradation (Figure 1).  
53 Whereas the contributions of  $RSLR$ ,  $Waves_{cross}$ , and  $Q_{anthrop}$  to shoreline change have, to date, attracted most of  
54 the attention of the coastal scientific community, the present study focusses on the relatively overlooked land-  
55 sea sediment pathway contribution  $\Delta Q$ .



56

**Figure 1.** Schematic representation of the river-wave sand transport. Diagram of the sand budget at the coast for one coastal cell (centred on one solid black ellipse). The sand supplied by the river ( $Q_{river}$ ) is re-distributed by wave-induced longshore transport ( $Q_{wave,in}$ ). Sand is lost or gained at any point through longshore transport ( $Q_{wave,out}$ ). A positive or negative budget is indicative of an accreted or depleted sediment budget at the coast, respectively.

57 On a global basis, there is a permanent flow of sediment from watersheds to the ocean, delivered by rivers  
58 (e.g., Syvitski and Milliman, 2007; Milliman and Farnsworth, 2011; Owens, 2020; Syvitski et al., 2022a). While the  
59 finer sediment particles, including silt and clay, reaching the sea are generally trapped in estuaries, deltas and  
60 low-energy embayments or transported far offshore, bedload transported from river mouths to adjacent coasts  
61 is the main source of terrigenous sediment supply to beaches. Of the estimated 7.5 Gt/yr of current sediment  
62 supplied by rivers to the global ocean (15.5 Gt/yr in 1950), 7.2 Gt/yr are suspended sediments (14.5 Gt/yr in 1950)  
63 while bedload constituted only 0.3 Gt/yr (1.0 Gt/yr in 1950) (Syvitski et al., 2022a). Based on a simple predictive  
64 model, Cohen et al. (2022) indicate a median proportion of bedload to total terrigenous material of about 15%,  
65 with a median particle size of 0.3 mm, with a fining trend with river size. If anything, this relatively modest figure  
66 for bedload, which concerns both sand and gravel, places into a sharp perspective the relatively low global  
67 availability of fresh fluvial bedload supply to maintain the world's beaches. Sand is described as being transported  
68 to the coast as bedload. Literature shows that suspended sand transport is generally equal to or greater than  
69 bedload for littoral grains (Camenen and Larson, 2005). We may reasonably assume that much of the load actually  
70 transported alongshore concerns sand because of the propensity for gravel to accumulate in storm-dominated  
71 high-latitude beaches close to river and glacial-till sources. Sediment supply from coastal erosion, erosion or  
72 reworking of sand-rich coastal deposits such as beach-ridges and dunes, as well as poorly consolidated soft-rock  
73 coasts, has been estimated at  $> 0.5$  Gt (Syvitski et al., 2022a; Regard et al. 2022) - undifferentiated mud and  
74 coarser sediment- and is commonly a source of gravel as much as sand. The production of sand from offshore  
75 carbonate factories (Laugié et al., 2019) is considered highly variable, with some coasts being richly supplied and



76 others having little or no carbonate supplies (Anthony and Aagaard, 2020). Offshore sources potentially involve  
77 the reworking of relict shelf-deposited terrigenous sediments or abandoned river-delta lobes subsisting on the  
78 shoreface. The longshore transport of sand, whatever the source, is of paramount importance to the stability of  
79 beaches. Additionally, the longshore transport system can also redistribute shoreface-derived carbonate and  
80 detrital (mainly quartz) sand as well as sand inputs from coastal erosion or reworking of sand-rich coastal deposits  
81 such as beach-ridges and dunes.

82 Wave-driven longshore sediment transport can conceptually be viewed in terms of a sediment cell with a  
83 budget involving inputs and outputs, the latter of which can be redirected towards the building of dunes or beach  
84 ridges. Some sand can be permanently lost into submarine canyons (Mazières et al., 2014), while severe storms  
85 can lead to prolonged and even permanent offshore losses (Gillet et al., 2008; Anthony and Aagaard, 2020). A  
86 sediment cell is an area of coastline where sand generally flows alongshore in a single direction (e.g. see Vitousek  
87 et al., 2017; Van Rijn, 2011). The balance of sand available for beaches at any time is the amount of sand entering  
88 the sediment cell minus the amount leaving (Figure 1). If this sand balance is altered, the beach sand budget and  
89 morphology will change. These aspects can be viewed in terms of alongshore sediment connectivity (Pearson et  
90 al., 2020) and its potential perturbation by engineering works, for instance (Cowell et al., 2003; Anthony, in press).

91 The proliferation of river management schemes for various purposes (Best, 2019), notably the construction of  
92 dams for hydropower generation and irrigation, and dikes and peripheral works for navigation and flood control,  
93 is increasingly leading to river fragmentation (Grill et al., 2019). Already perturbed river sediment fluxes are  
94 further relayed by massive sand extractions in river beds (Peduzzi, 2014; UNEP, 2019). Along the coast, sediment  
95 fluxes are increasingly impacted by engineering structures to control erosion and with the development of  
96 harbours (Pilkey and Cooper, 2014; Abessolo et al., 2021; Anthony, in press), further depriving beaches distant  
97 from river outlets of an essential supply of sand (Syvitski et al., 2003; Wiegand, 1996; Milliman and Farnsworth,  
98 2011; Yang et al., 2011). At the same time, the rate of sea-level rise is projected to accelerate over the 21<sup>st</sup> century  
99 (Oppenheimer et al., 2019; Fox-Kemper et al 2021), compounding the current problems.

100 While coastal sand pathways and associated sediment cells have been abundantly addressed at local and  
101 regional scales (Abam, 1999; Anthony et al., 2019; Bamunawala et al., 2021; Warrick et al., 2020), they have not  
102 received attention from the coastal engineering/scientific community at the global scale. There is, however, a  
103 need for a comprehensive consideration of global sand availability to coasts and its alongshore redistribution  
104 pathways if we are to find ways of effectively anticipating and eventually mitigating the effects of climate change  
105 on beaches as well as the consequences of increasing human interventions on alongshore sand mobility. Recent  
106 developments in remote sensing (Benveniste, et al., 2019; Melet et al., 2020) provide scope for the generation of  
107 global databases, for instance, on the distribution of sandy beaches (Luijendijk et al., 2018), sub-aerial beach  
108 slopes (Vos et al., 2020), nearshore slopes (Athanasiou et al., 2019), and shoreline change (Mentaschi et al., 2018;  
109 Luijendijk et al., 2018). However, while being part of the way forward to improve science-based coastal  
110 management strategies, these environmental databases need to be carefully considered in the light of realistic  
111 scenarios and models. The purely data-derived information in these databases needs to be carefully used, while  
112 considering physical processes as well. For a holistic consideration, it is necessary to gain insight on how the  
113 combination of terrigenous sand supply from rivers, and coastal redistribution of this supply, link with sandy  
114 beach evolution at the global scale. With that goal, we introduce here an integrated sand pathway model and



115 quantify the impact of river-basin changes on modern-era coastal sand budgets often far from the rivermouth  
116 and the observed retreat affecting nearly a quarter of the world's sandy beaches.

## 117 **2 Data and Methods**

### 118 **2.1 The global sand pathway model**

119 A numerical 'along-coast' sand transport model has been developed and implemented on the world's coastline  
120 segmented into  $0.5^\circ$  alongshore cells, applied in a stationary mode (i.e. no time step). The terrigenous sand  
121 budget of each of the 11,161 coastal cells is calculated considering the sediment conservation equation 1 (Figure  
122 1) for either side (alongshore) of the cells and from the shoreline to the depth of closure (cross-shore, see  
123 Hallermeier, 1978; Bergsma and Almar, 2020). The source term  $Q_{river}$  corresponds to the bedload discharge by  
124 rivers (1.0 Gt/yr in 1950, 0.3 Gt/yr of bedload in the present period, see Milliman and Farnsworth, 2011 and  
125 Syvitski et al., 2022a), of which only a fraction is sand (including gravel but discarding mud). The wave-induced  
126 longshore sand transport, the predominant sand transport mode along open, wave-exposed coasts, is  
127 represented by  $Q_{wave}$  (Kamphuis, 1991). This transport occurs mostly in the surf zone which generally extends  
128 offshore for tens of metres to a couple of hundreds of metres. Each of these sediment fluxes relies on different  
129 physical mechanisms and thus requires a large amount of data to be estimated. Here,  $Q_{river}$  is calculated at each  
130 coastal cell from river watershed mean inputs, in this case for the years 1980-2010, from a calibrated erosion law  
131 (BQART or Maffre's formulae, cf. Sect 2.3) depending on the catchment area, mean annual catchment discharge,  
132 average temperature and local slope (Syvitski and Milliman, 2007; Maffre et al. 2018). To verify the soundness  
133 of this calculation, we compared our estimate to Milliman and Farnsworth's (2011) database, obtaining a good  
134 agreement (Supplementary Section S1, Figure S1).  $Q_{wave}$  is calculated from climatological ocean data (over the  
135 1993-2015 period) such as wave height, wave period, and wave orientation relative to the coast (Kamphuis, 1991,  
136 see Sect 2.4 for a sensitivity analysis on the choice of the formulation).

137 This model produces patterns in coastal sand accumulation and removal, i.e. accreted or depleted volumes.  
138 We do not go on to predict sandy morphological change, i.e., coastal advance or retreat, strictly speaking, because  
139 conversion of the calculated accumulation/removal volumes into morphological change would require taking into  
140 account an additional level of complexity due to accommodation space modulated by relative sea-level changes  
141 (e.g. sea-level rise, subsidence affecting coastal bathymetries that still remains to be mapped adequately at the  
142 global scale) and morphodynamic considerations (e.g., beach profile evolution, dune accretion), which entail  
143 uncertainties not relevant to the specific question addressed here. The ability of our sand pathway model, leading  
144 to coastal sediment imbalance, and potentially to shoreline migration, is tested against shoreline change  
145 observations by Luijendijk et al. (2018).

### 146 **2.2 Global coastal cells**

147 For the coastline grid points, we use the Global Self-consistent Hierarchical High-resolution Geography  
148 Database (GSHHG version 2.3.6 August 17, 2016; Wessel and Smith, 1996). The GSHHG coastline is further  
149 segmented into coarser points with a  $0.5^\circ$  alongshore ( $\sim 50$ -km) resolution and called cells (Almar et al., 2021).  
150 Locations at latitudes above  $50^\circ$  north and south were excluded as they correspond to areas such as Patagonia



151 or Northern Canada where the model fails to properly represent sand transport, probably due to the multitude  
152 of closely interspaced islands. Also ERAInterim wave model struggles with ice caps.

## 153 2.3 River sediment supply

### 154 2.3.1 BQART

155 The annual river sediment discharge, represented by the variable  $Q_{river}$ , was calculated over the 1979-2015  
156 period from river watershed coastal points and interpolated at each coastal cell using the widely used BQART  
157 formula (Syvitski and Milliman, 2007, see Equation 3). We used it for every watershed connected to the ocean,  
158 as defined in the HydroBASIN database (Lehner et al., 2013). Regarding the size of watersheds for which BQART  
159 is valid, recent work indicates that BQART may not be applicable to small watersheds more exposed to singular  
160 behavior such as extremes (Warwick et al., 2022, 2023). Of note, Syvitski et al. (2022b) indicate that small basins  
161 contribute only very little fluvial sediments. In the HydroBASIN database, small streams that drain directly to the  
162 coast are aggregated into larger entities of the order of  $100 \text{ km}^2$  (max  $500 \text{ km}^2$ ). In the absence of a better solution,  
163 we applied BQART on these surfaces.

$$164 \quad Q_{river} = \omega B Q^{0.31} A^{0.5} R \times \max(T, 2) \quad (3)$$

165 where  $\omega = 0.0006$  (Syvitski and Milliman, 2007),  $Q_{river}$  is the sand river discharge in  $Mt/year$ ,  $T$  is the average  
166 ambient temperature ( $^{\circ}C$ ),  $Q$  is the liquid river discharge ( $km^3/year$ ),  $A$  is the drainage area of the catchment ( $km^2$ )  
167 and  $R$  is the relief (i.e. the difference in elevation from highest catchment point and its outlet, in  $km$ ). In addition,  
168  $B = IL(1 - Te)E_H$  accounts for geological as well as human factors (Syvitski and Milliman, 2007). In the formulation  
169 of  $B$ ,  $I$  is a modulation from glacier erosion:  $I = 1 + 0.09A_g$  where  $A_g$  is the percentage area covered by glaciers.  $L$  is  
170 a lithological factor usually in the range of 0.5 (low erodibility lithology) to 3 (high erodibility lithology).  $Te$  is the  
171 fraction of potential sediment retention in plains, lakes, whether natural or anthropogenic – i.e. dams; it ranges  
172 between 0 and 1, with 1 representing complete retention. This parameter is poorly constrained. Due to missing  
173 regional information, here the same value was used for all the catchments and corresponds to a worldwide mean  
174 of 0.2 (Syvitski and Milliman, 2007). Last,  $E_H$  is an anthropic factor, and can have one of three possible values  
175 (Syvitski and Milliman, 2007):  $E_H = 0.5$  for areas with conservative human footprints (density  $< 200 \text{ inh./km}^2$ , and  
176 gross domestic product per capita  $> 15000 \text{ \$/yr}$ );  $E_H = 2$  for areas with high human footprints (density  $> 200$   
177  $\text{inh./km}^2$ , and gross domestic product per capita  $< 1000 \text{ \$/yr}$ ); or  $E_H = 1$ , for areas with low human footprints.

178 In order to calculate  $Q_{river}$  at the coast for all catchments with the BQART formula, we extracted the values of  
179  $Q$ ,  $A$ ,  $R$ ,  $T$ ,  $A_g$ , population density, and gross domestic product per capita from the HydroBASIN database (Lehner  
180 et al., 2013).  $L$  is determined from the *lit\_cl\_smlj* categories in the GLiM database (Hartmann and Moosdorf, 2012).  
181 A validation to this BQART model was conducted with data from Milliman and Farnsworth (2011) and discussed  
182 in Supplementary Section 2.

### 183 2.3.2 Maffre's model

184 Alternatively to the BQART, and in order to better evaluate the potential impact of terrestrial retention such  
185 as with dams on the sand flux in different catchments, we used a model where the sediment flux can be calculated  
186 on every pixel and either summed or partially removed by dams in order to calculate the sediment outflux to the



187 ocean  $Q_{river}$ . This model was proposed by Maffre et al. (2018) on the basis of a  $3.75^\circ$  longitude by  $1.9^\circ$  latitude  
188 grid of cells:

$$E = kq^{0.2}s^{1.3} \times \max(T, 2)^{0.9} \quad (4)$$

189  
190 where  $E$  is the pixel erosion rate in  $m/year$ ,  $k$  is a constant parameter adjusted to obtain a global sediment outflux  
191 of 19 Gt (as predicted by the BQART model),  $s$  is the local slope,  $q$  is the run-off ( $mm/year$ ) and  $T$  is the ambient  
192 temperature in ( $^\circ C$ ). Erosion rates are summed within catchments in order to predict the sediment flux  $Q_{river}$  at  
193 their outlet. The results of BDART and Maffre models illustrated present a good agreement (Figure S2).

### 194 2.3.3 Dam impact

195 To quantify the impact of dams in  $Q_{river}$ , we used the GOODD dam database (Mulligan et al., 2020), which  
196 provides the location of the dams as well as the associated upstream watersheds. We calculated  $Q_{river,dam}$  by  
197 masking the area upstream from the dams, so that it mimics total sediment retention in dam reservoirs assuming  
198 that 100% of the sediment is trapped. Overall,  $Q_{river,dam}$  fits  $Q_{river}$  calculated by using the BQART with a correlation  
199 coefficient of  $R = 0.76$ . To investigate the influence of potential impact on river catchments, we also calculated  
200 an unrealistic pristine potential  $Q_{river,p}$  assuming a world without artificial river catchments (i.e. dams) and using  
201 Equation 3, so that we can compare the two situations with respect to the sandy coast evolution. Because our  
202 model focuses on sand, we consider that only a fraction (e.g. an arbitrary 35% value was used here, but values as  
203 low as 10% are found in the literature) of the total riverine sediment input is sand reaching the coastal zone  
204 (Wright and Nittrouer, 1995). A sensitivity analysis is shown in Figure S5 and discussed in Supplementary Section  
205 S4 and shows that our conclusions are rather insensitive to this fraction, and also to sediment grain size, which  
206 may vary with water shed and soil/land characteristics.

## 207 2.4 Longshore wave-induced sand transport

208  $Q_{wave}$  is calculated at every single cell, in a stationary model. To do so, there are several bulk longshore sand  
209 transport formulations that are widely applied by coastal engineers. These are, among others, the CERC (1984),  
210 Kamphuis (1991), and the more recently developed Kaczmarek et al., (2005) formulae. There are continuous  
211 research efforts on the improvement of bulk longshore sediment transport equations (see for example, Mil-  
212 Homens et al., 2013) yet there is no general consensus on the choice of a formulation. The sensitivity analysis of  
213 our results to the choice of the formula in Supplementary Section 3 shows no clear difference on a global basis  
214 (Figure S2). Here, the empirical wave-induced longshore sediment transport is based on hydrological and  
215 topographic data and calculated using the Kamphuis formula (Equation 5) which shows a good agreement when  
216 compared with ground truth at several sites worldwide (Figure S3):

$$217 \quad Q_{wave} = 2.33T_p^{1.5} \tan(\beta)^{0.75} d_{50}^{-0.25} H_{break}^2 \sin(2\theta_{break})^{0.6} \quad (4)$$

218 We consider a single grain size of  $d_{50} = 400 \mu m$  (see the sensitivity test in Figure S5) which corresponds to  
219 intermediate medium-sized sand (ranging from fine –  $60 \mu m$  up to coarse  $1000 \mu m$   $d_{50}$ , e.g. see Flemming, 2011),  
220 with a surf zone of  $\tan(\beta) = 0.1$  (Ardhuin and Roland, 2012; Melet et al., 2018). More advanced foreshore slope  
221 data are becoming available all over the world (e.g. from Almar et al., 2021b; Athanasiou et al 2019), but still with  
222 substantial discrepancies relative to ground truth in the surf zone. In Eq. 5,  $T_p$  is the peak wave period in  $s$ ,  $H_{break}$



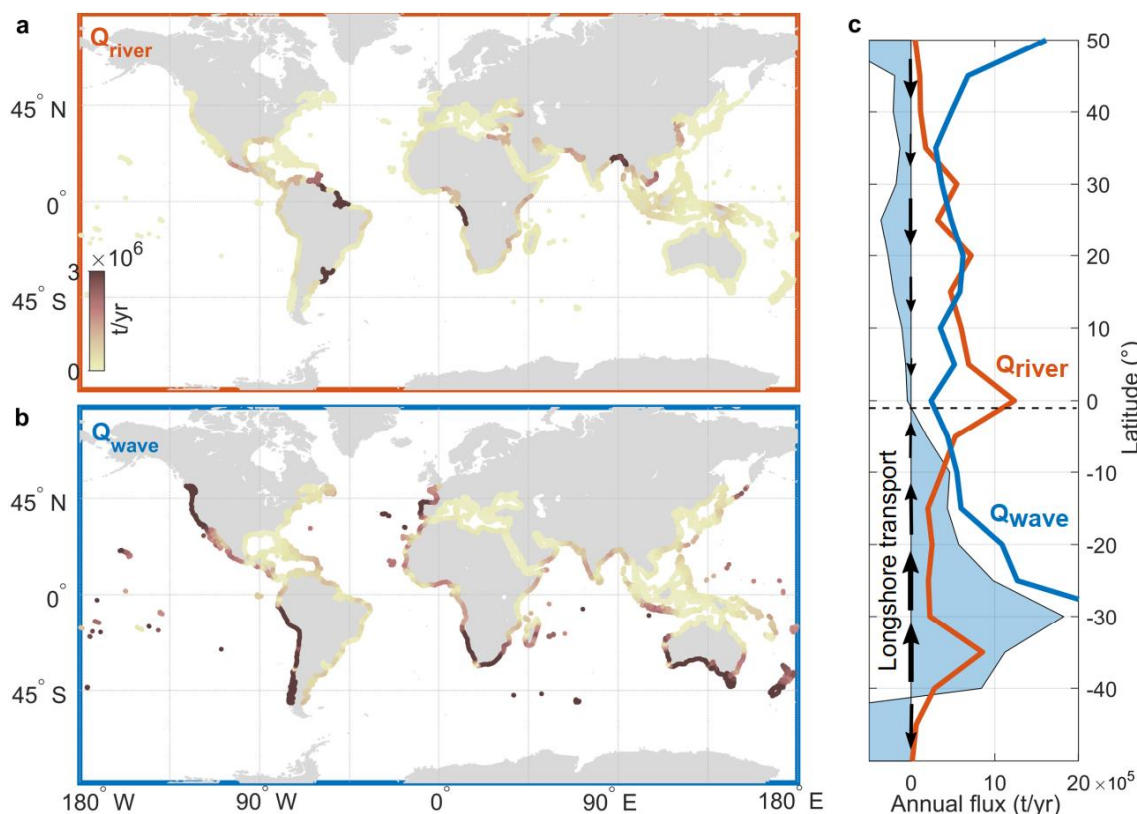
223 the wave height at the breaker line (in  $m$ ) and  $\vartheta_{break}$  the wave angle at the breaker line in degrees. The average  
224 wave regime was derived from ERA-Interim (ECMWF) over the 1993-2015 period. We did not account for the  
225 transformation of waves from offshore deep waters to the continental shelves and coastal zones, a process that  
226 can be substantial with wide continental shelves (Passaro et al., 2021). The sensitivity of our global model and  
227 the longshore sand transport to sediment grain size and coastal slope is discussed in Supplementary Section S4.  
228 Figure S5 indicates no substantial change of model score and when varying  $d_{50}$  and coastal slope, as the model  
229 looks at patterns not the values themselves that might be influenced.

230 According to the relative angle between the waves and shoreline, transport occurs in one direction or the  
231 other. A set of consecutive cells where the transport moves in the same direction constitutes a coastal cell. Within  
232 a cell, each cell receives sand from the previous cell and supplies sand to the next cell. A positive/negative  $\Delta Q_{wave}$   
233 across a cell is indicative of accretion/erosion. When Islands are considered as isolated coastal systems, there is  
234 no sand flux from one island to another. The model provides results in one iteration starting from a hypothetical  
235 initial situation where sandy beaches are infinite reservoirs of detached sand and non-sandy stretches of coast  
236 are empty reservoirs. Here, the sandy cells were delineated as in the database of Luijendijk et al. (2018).

### 237 3 Coastal sand mobility potential and Equator-ward convergence

238 The quantification of  $Q_{river}$  is well documented locally at the outlets of the world's major rivers (Milliman and  
239 Farnsworth, 2011; Besset et al., 2019). It is then possible to integrate this output over large areas (e.g. a continent)  
240 and at the global scale (Milliman and Farnsworth, 2011, Syvitski and Milliman, 2007). Using the widely used  
241 BQART model (calibrated with rivers data Supplementary data S1), here with pristine watersheds without human  
242 dams, at the global scale gives a total annual sediment flux of  $\Sigma Q_{river} = 15.1$  Gt/yr (over the 1980-2010 period),  
243 which is within the already estimated pristine range of 10 to 20 Gt/yr (Syvitski and Kettner, 2011; Dedkov and  
244 Gusarov 2006 ; Peucker-Ehrenbrink, 2009).  $\Sigma Q_{river}$  corresponds thus to  $5700 \times 10^6$  m<sup>3</sup>/yr considering  $\rho_s = 2650$   
245 kg/m<sup>3</sup>. Integrated over all the coastal cells, this gives an average of 1,050,000 tons per year per cell, or 400,000  
246 m<sup>3</sup>/yr per cell. All this global sediment flux can be reconsidered and brought down to bedload, and sand only,  
247 discarding the finer fraction of suspended sediment such as mud (Figure 2).

248  $Q_{wave}$  is an estimate of the potential (i.e. maximum) annual flux of sediment transport along the coast driven  
249 by waves. On a global basis, the longshore sediment transport potential per cell is approximately 155,000 cubic  
250 meters (410,000 tons) per year, when averaged over the 1993-2015 period. The value closely aligns with  
251 terrestrial discharge, unveiling significant potential for wave-driven remobilization and redistribution along the  
252 coast. In Figure 2, the global latitudinal averages of  $Q_{wave}$  show a tendency for waves in the northern and southern  
253 hemispheres to transport sediment southward or northward, respectively. Around the Equator, the reversal of  
254 the direction of the longshore sediment transport potential represents a global convergence zone of these  
255 transport potentials. On average, at a global scale, waves appear to induce sediment transport from higher  
256 latitudes to the equatorial zone with notably high sediment deposition in tropical areas where there is a  
257 pronounced decrease in wave energy (Figure 2). Figure 2c shows that the relative importance of  $Q_{wave}$  and  $Q_{river}$   
258 depends on latitude. Between 15°N and 5°S,  $Q_{river}$  dominates over  $Q_{wave}$  whereas  $Q_{wave}$  dominates south of 10°S  
259 and north of 35°N.



260

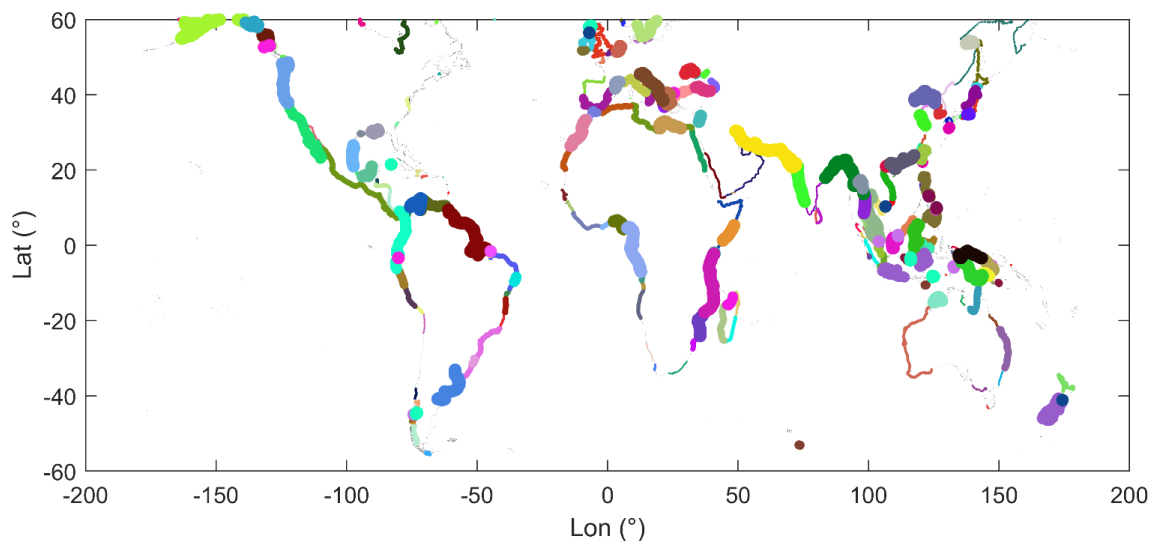
**Figure 2.** A global view of fluvial sediment sand supply and longshore sediment transport. (a) Global geographic distributions (along the set of cells delineated by GSHHG i) of the river sediment discharge ( $Q_{river}$ ) and (b) absolute longshore sediment transport potential ( $Q_{wave}$ ), with blue arrows indicating the general direction of transport. (c) 5° resolution latitudinal averages of  $Q_{river}$  (red line), absolute  $Q_{wave}$  (blue line) and directional  $Q_{wave}$  (blue polygons - positive for northward-oriented, negative for southward-oriented). Black arrows show the directions and intensities of the longshore sediment transport.

261 When  $Q_{river} < Q_{wave}$ , the river sediment supply is easily transported by  $Q_{wave}$ . Sediment deposition, and  
262 consequently, beach (if any) accretion, is expected where  $Q_{wave}$  diminishes alongshore. On the contrary, areas  
263 where  $Q_{river} > Q_{wave}$  may be dominated by large river bedload discharge, locally outweighing  $Q_{wave}$ , which means  
264 that most of the sediment supplied is either deposited near the river mouth (sequestered in river deltas, for  
265 instance, including subaqueous delta fronts that may protrude far offshore). From 25°N to 0°, there is a consistent  
266 decrease in the mean southward (northward) coastal sediment transport, whereas from 30°S to 0° the northern  
267 component of sediment transport tends to decrease. This gradient of transport capacity leads to a progressive  
268 deposition of sediments, especially in tropical areas where this trend is most pronounced.



269 The impact of river discharge is often discussed locally, specifically around the outlets and in particular at  
270 deltas (Nienhuis et al., 2020). However, sediment has the potential to travel across the entire sediment cell, which  
271 can span thousands of kilometers along the coast. A sediment cell represents a coastal stretch that shares  
272 common characteristics in terms of sediment nature and how it moves over space and time. Any disturbance  
273 occurring upstream of the sediment flux will affect the downstream portion. Figure 3 illustrates the computed  
274 sediment cells, showcasing their shared temporal variability with a 0.8 correlation threshold value. Large  
275 sediment cells are observed at open and continuous stretches of coast such as Pacific coast of South America and  
276 Atlantic coast of South Africa till the Congo plain meanwhile smaller cells are observed at more rugged coasts  
277 such as in Indonesia archipelago, Caribbean and Europe. Meanwhile, the length of these cells is sensitive to the  
278 chosen threshold with average values up to 2000 km. This sensitivity is attributed to the variation in  
279 convergence/divergence points, such as headlands and bays, in the longshore sediment transport, which tends  
280 to increase with higher resolution and a decrease in the threshold value.

281



282

283

284 **Figure 3.** Distribution of coastal sediment cells based on the continuity of longshore sediment transport.  
285 Colours are illustrative to visually distinguish the different zones and do not reflect a particular value.  
286 Line width is proportional to fluvial sediment income in each coastal sediment cell.

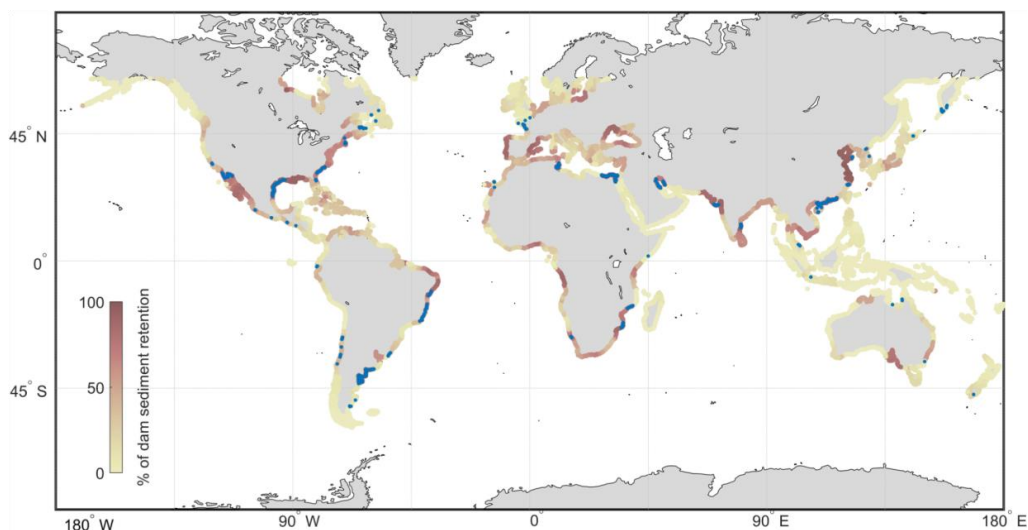
#### 287 **4 Potential reduction of terrestrial sediment supply by rivers: the key influence of** 288 **dams**

289 In the above analysis, pristine natural watersheds were used (as in Syvitski and Milliman, 2007). This is  
290 arguably a large simplification of the problem. Significant emphasis has been placed on the impact of



291 anthropogenic activities on river sediment supply (Syvitski and Milliman, 2007; Milliman and Ren, 1995;  
292 Ranasinghe et al., 2019). The effect of human-induced modifications of river loads has also been recognized in  
293 numerous individual beach studies worldwide (Bamunawala et al., 2020, 2021). Note that dam trapping is only  
294 part of the problem and that river-bed mining is also a very important activity (Peduzzi, 2014; UNEP, 2019), with  
295 deleterious effects on the coastal sediment budget. Changes in precipitation and land have been reported to have  
296 also an important contribution to sediment discharges.

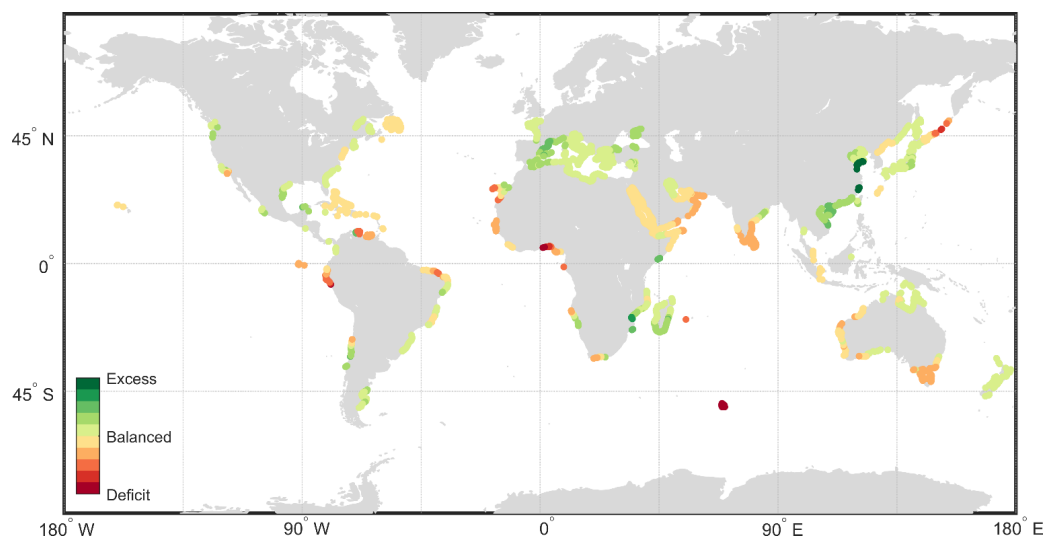
297 In order to move beyond case studies, here we assess specifically the global picture of anthropogenic effect  
298 of dam trapping. In the BQART formula, dam trapping anthropogenic effect can be reflected by the  $T_e$  term.  
299 However, BQART is not suited to account for the influence of river dams because it is integrated over all the  
300 watersheds, and we preferred the Maffre's model (see Sect 2.3.2) where the sediment flux can be calculated on  
301 every pixel of the catchment and either summed or partially removed by dams in order to calculate the sediment  
302 outflux to the ocean  $Q_{river}$ . In the dam scenarios adopted here, the two models are end-members with full or no  
303 dam trapping. The model with dams retaining 100% of sediment is extreme, as, in reality, the sediment trapping  
304 efficiency is quite variable, mainly depending on the water residence time (Maneux et al., 2001; Tan et al., 2019),  
305 and only sometimes up to 100% (example of the Aswan Dam on the Nile; Walling and Webb, 2009). The difference  
306 between these two scenarios is shown in Figure 4. Figure 4 shows that a potential dam retention capacity of 100%  
307 of sand would reduce the overall  $Q_{river}$  by half, from 600,000 cubic metres per year per cell in a pristine world to  
308 270,000 cubic metres per year per cell on average in a world where dams retain all the bedload, thus depriving  
309 sandy coastal systems of half of their natural terrigenous sediment supply. Note that these extreme values  
310 bracket the current value estimated (400,000 cubic metres per year per cell). In this tested scenario, 18 % of the  
311 sandy cells (i.e. approximately 180,000 km of coastline) with a neutral or positive sand budget in a pristine  
312 situation become sediment-deficient once total retention by dams is assumed (orange/red locations in Figure 5),  
313 often far from the outlet. Although extreme, this scenario illustrates the potential effect of dams and provides  
314 pertinent information on the locations of coastal areas affected (or that may be affected) by fluvial sediment  
315 input losses (Figure 5).



316



**Figure 4.** Potential dam-induced reduction of fluvial sediment supply to the world's coasts from pristine world, here shown in percentage of decrease in  $Q_{river}$  induced by dams, assuming that dams retain 100% of the bedload coming from upstream using Maffre's model and GOODD dam database (Mulligan et al., 2020). The blue dots represent cells where the sand budget balance turns from positive to negative when dams are taken into account.



317

**Figure 5.** Coastal sand budget change for all sandy locations, between no retention and total retention scenarios. Traffic light system representation from potential large deficit (-500,000 t/yr) to large excess (+500,000 t/yr).

321 In order to evaluate our sand pathway model, we compare the pattern given by several scenarios of coastal  
322 sediment balance results with available observations for global coastline mobility; pristine sediment ( $\Delta Q_{pristine}$ )  
323 and dam ( $\Delta Q_{dam}$ ) pattern. Here, we tested the correlation ( $R$ ) between the observed annual coastline evolution  
324 trend  $U_{obs}$  and our calculated  $\Delta Q$ . Sandy points are categorized using Luijendijk et al. (2018) and the dominance  
325 of not sandy/sandy is explored regionally (length scale of  $4^\circ \sim 400$  km). For all sandy points (31% of the total  
326 coastal points), the correlation coefficient between  $U_{obs}$  and  $\Delta Q_{dam}$  is  $R = 0.49$  for sandy coastline, showing the  
327 preponderant influence (34% on a global basis) of river damming alone on explaining current sandy beaches  
328 evolution trend. The significant correlation between  $\Delta Q_{dam}$  and  $U_{obs}$  for a majority of global sandy beaches shows  
329 that our sand budget model captures, to first-order, the current cross-shore mobility of sandy shorelines, only  
330 due to the local imbalance between fluvial sediment supply and the sediment-carrying capacity of wave-induced  
331 longshore currents. Thus, the fate of river sand supply cannot be neglected when considering the cross-shore  
332 evolution of sandy beaches, especially at decadal time scales as considered here, and even at distance from  
333 outlets.

334 Fluvial sediment loss has in fact already been shown to be critical to deltas, especially large deltas, which are  
335 becoming increasingly vulnerable as a result of sediment depletion compounded by anthropogenic subsidence



336 (Syvitski et al., 2009; Besset et al., 2019; Dunn et al., 2019; Ranasinghe et al., 2019). Large rivers deliver much of  
337 the fluvial load to the oceans, with only 1052 rivers delivering 95% of the total (Syvitski et al., 2022b). Thus, the  
338 construction of dams that essentially trap bedload has extremely deleterious effects by undermining not only the  
339 stability of sandy beaches adjacent to deltas but also the rest of the world's sandy beaches sourced by terrigenous  
340 sediment transiting through river mouths.

## 341 **5 Beach conservation**

342 Our results show that a primary global threat to sandy coasts may arise from fluvial sediment supply deficit. A  
343 number of examples have shown that sandy coasts can be rapidly reconstructed after river dam removal (Warrick  
344 et al., 2019). However, such actions must be based on conservation and integrated management policies, a trade-  
345 off at the nexus of sustainable coastal areas (Nittrouer and Viparelli, 2014; Dada et al., 2021).

346 Past experience has shown that effective, site-specific coastal planning can mitigate beach erosion and result  
347 in a stable coastline; the most prominent example of this is the Dutch coast (Mulder et al., 2011). While sea-level  
348 rise is projected to result in shoreline retreat almost everywhere in the world (IPCC, 2021), many locations have  
349 ambient erosive trends related to human interventions that could theoretically be avoided by more sustainable  
350 coastal and watershed management practices (Morris et al., 2020; Lincke and Hinkel, 2021; Vousdoukas et al.,  
351 2020, Luijendijk et al., 2018). At the same time, projected sea-level rise implies unprecedented pressure on our  
352 coasts, requiring the development and implementation of informed and effective adaptation measures (Pörtner  
353 et al., 2022). At local scales, human activities can also directly affect the coastline, both in terms of erosion and  
354 accretion. Some countries such as the Netherlands or China are undertaking large-scale works to gain ground on  
355 the sea. Others use their beaches as sand quarries to supply the construction industry. Land subsidence due to  
356 agriculture, mining, or urban development (Nicholls et al., 2021; Marchesiello et al., 2019), as well as coastal  
357 infrastructure, can be a dominant factor in coastal evolution (Cao et al., 2021). This was recently highlighted by  
358 the decision to move the capital city of Jakarta due to the perceived impossibility of sustainably protecting it from  
359 marine flooding (Cao et al., 2021).

360 However, most of these site-specific mitigation efforts have neglected the sediment imbalance that results  
361 from larger-scale, often regional, sediment redistribution (Almar et al., 2015). Our study strongly suggests that  
362 efficient management strategies cannot be limited to just coasts but should consider entire river basins within a  
363 more holistic treatment of the problem. Modification of the sediment supply by a river, which may even run  
364 across several countries, can have repercussions along the coast for up to more than a thousand kilometres (e.g.  
365 the Namibian coast), depending on the size of the coastal sediment cell. For example, the Bight of Benin, located  
366 in the Gulf of Guinea, West Africa, is under the influence of sediment supplied by the Volta and Niger rivers, and  
367 this sediment is redistributed along hundreds of kilometers of coast (Anthony et al., 2019; Abessolo et al., 2021).  
368 However, several agriculture and hydro-power dams have been constructed along these rivers, as well as  
369 deepwater harbours, blocking both river-to coast sediment transport as well as alongshore transport (Anthony  
370 et al., 2019). Although some countries are implementing expensive management strategies locally, a  
371 collaborative regional international effort would certainly deliver more benefits (Dada et al., 2021; Alves et al.,  
372 2020) at a reduced cost (Rocle et al., 2020). Current legislation does not take the integrated analysis of continental  
373 and offshore sources of sediments into account, but our study suggests that it is possible to act on saving sandy



374 coasts by assuring the sediment balance, for example, via implementing innovative strategies of sediment  
375 management in the wake of retention by dams, better control of riverbed mining, and adapting land-use policies  
376 at a regional-to-continental scale, an approach that requires particular coordination for trans-boundary rivers (De  
377 Stefano et al., 2017) . National initiatives, mainly founded on dam removal, have already been launched, notably  
378 in the United States, Japan and Europe (Warrick et al., 2019; Noda et al., 2018; Habel et al., 2020). The need for  
379 a stronger dialogue between the scientific and public domains on the impacts of dams has been advocated  
380 (Flaminio et al., 2021). Such knowledge transfer and exchange are not only beneficial regarding, for example,  
381 perceptions of 'renewable energy' and 'green energy,' but also in terms of consideration of alternative modes of  
382 governance regarding dams. Given that the change in sediment outflow from one river may impact the shorelines  
383 of another country, we anticipate that integrated and comprehensive approaches such as advocated here could  
384 have major benefits both for national coastal management policies and for regional international legislation.

## 385 **6 Discussion**

386 In this global study, we have necessarily made approximations and assumptions. We limited our analysis to  
387 the potential sand pathway from land to sea and the alongshore redistribution by waves, and did not consider  
388 offshore sediment export beyond the depth of closure, nor sand inputs from offshore sources, which are out of  
389 the scope and reach of our study. The analysis used both sandy locations and shoreline change metrics from  
390 Luijendijk et al. (2018) which is a first-pass pioneering estimate and can be obviously refined using new  
391 classification tools, including machine learning (Vos et al., 2019).

392 Regarding the direct influence of dams, a river sand flux dropping to nearly zero can be attributed primarily to  
393 the impact of dams. However, the effect of water extraction from the reservoir also plays an important role on  
394 downstream erosion. For example, due to water extraction, the Nile river water discharge to the sea has  
395 decreased to nearly zero after the construction of the Aswan dam (Wiegel, 1996). No water discharge means no  
396 sediment delivery. But no water discharge also means no downstream erosion. In the Yangtze River, the sediment  
397 flow to the sea after the closure of the Three Gorges Dam remained at about 25%, as the water flow was hardly  
398 affected and river erosion downstream of the dam was still considerable (Yang et al., 2018). However,  
399 consideration of such phenomena is beyond the scope of our study. The reality lies in between our two extreme  
400 scenarios (0% or 100% retention of sediments in the dams). The temporal evolution of coastlines and its feedback  
401 on waves and the longshore sediment transport was not accounted for in our study. Numerous articles document  
402 this feedback by waves in reshaping the delta coastline (Anthony, 2015; Nienhuis et al., 2015), for instance at the  
403 Mekong (Marchesiello et al., 2019) and the Volta river deltas (Anthony et al., 2016). We believe this aspect, which  
404 involves coastline evolution and its feedback on waves, is currently out of the reach of our methodology,  
405 especially at global scale.

406 Although the sand budget plays a primary role in the evolution of the coastline on a global scale, other  
407 phenomena, natural or not, can influence this evolution on different spatial and temporal scales. The contribution  
408 of these phenomena is difficult to quantify because global databases (e.g. high-resolution offshore bathymetric  
409 data or a subsidence map) are still lacking. Among these various phenomena, the global rise in sea level over the  
410 last 100 years has had a visible impact on beaches, especially along gently sloping low-lying coasts. With a ~ 20  
411 cm rise in the sea level since 1900 (Oppenheimer et al. 2019), the sea has gained up to 15 metres on land for



412 beaches with a slope of 1 degree. Local subsidence due to sediment compaction following freshwater pumping  
413 can reach several metres as in Japan or Indonesia (Cao et al., 2021; Tay et al., 2022), greatly exceeding any other  
414 cause for coastline evolution. Abrupt, or progressive or transient vertical uplift or subsidence on the scale of  
415 centimetres to metres over a period of years can locally influence the relative sea-level rise substantially (e.g.,  
416 Jeanson et al., 2021), and consequently the coastline position (Farías et al., 2010). These phenomena are not  
417 quantified everywhere and may explain the remaining variance in the current sandy beach trend  $u_{obs}$  that is not  
418 explained by  $\Delta Q$ .

419 Nevertheless, our study constitutes a major breakthrough by providing the first evidence that the current  
420 trend in sandy coastal evolution is controlled by the local imbalance of sand transport in a predictable way.  
421 Sediment supplied by rivers plays a crucial role in this imbalance and any variation in this supply, caused by dams  
422 or aggregate extractions for example, can affect sediment redistribution along continental cells. Variations in the  
423 river sediment supply are also affected by climate change. The rise in temperature (Hoegh-Guldberg et al., 2018)  
424 will increase the sediment transport potential of rivers as temperature directly affects the capacity of the river to  
425 erode the bed (Syvitski and Milliman, 2007). The intensification (reduction) of precipitation in temperate (arid)  
426 zones will lead to an increase (decrease) in  $Q_{river}$  (Greve et al., 2018). Last, the multiplication of extreme climatic  
427 events (i.e. droughts, extreme precipitation, extreme sea levels etc.) will increase vulnerability to erosion and  
428 thus influence sediment transport; for example, monsoon rains after a strong drought mobilizes large quantities  
429 of sediments. Dams are not the only anthropogenic factor to be considered with regards to the evolution of  $Q_{river}$ .  
430 Land use changes also have a critical role to play in the delivery of river sediment supply to the coast. Urbanization  
431 can hamper sediment transport, particularly through the increase in infrastructure along rivers and coasts.  
432 Conversely, deforestation and land use in general may also help increase  $Q_{river}$  by increasing the exposure of  
433 deforested soils to precipitation and the erodibility of soils that do not have enough tree roots to provide support  
434 (Restrepo et al., 2015; Ribolzi et al., 2017; Owens, 2020).

### 435 **Code availability**

436 The raw data that support the findings of this study are already available online. Calculated data (e.g. sediment  
437 outfluxes) are provided as tables. The Matlab Code will be made freely available through gitlab repository.

### 438 **Author contributions statement**

439 Conceptualization by VR and RA. MG carried out early stage study and wrote an initial draft under supervision  
440 by VR, RA and SC. VR and SC, and RA calculated the sediment supply from rivers at the global scale, and LST,  
441 respectively. PM brought his expertise on riverine fluxes. RA and VR directed the manuscript preparation. RR and  
442 EA strengthened the presentation through their external and wide expertise. All authors discussed the results  
443 and contributed to the manuscript.

### 444 **Competing interests**

445 The authors declare that they have no conflict of interest.

446



## 447        **Acknowledgements**

448        RR is partially supported by the AXA Research Fund

449

## 450        **References**

451        Abam, T. K. S. (1999). Impact of dams on the hydrology of the Niger Delta. *Bulletin of Engineering Geology and*  
452        *the Environment*, 57(3), 239-251

453        Almar, R. et al. Response of the Bight of Benin (Gulf of Guinea, West Africa) coastline to anthropogenic and  
454        natural forcing : Part 1 : Wave climate variability and impacts on the longshore sediment transport. *Cont. Shelf*  
455        *Res.* 110, 48 –59, DOI: 10.1016/j.csr.2015.09.020 (2015).

456        Abessolo, G. O., Larson, M., & Almar, R. (2021). Modeling the Bight of Benin (Gulf of Guinea, West Africa)  
457        coastline response to natural and anthropogenic forcing. *Regional Studies in Marine Science*, 48, 101995.

458        Alves, B., Angnuureng, D. B., Morand, P. & Almar, R. A review on coastal erosion and flooding risks and best  
459        management practices in West Africa : what has been done and should be done. *J. Coast. Conserv.* 24, art. 38 [22  
460        p.], DOI:

461        Anthony, E.J., Wave influence in the construction, shaping and destruction of river deltas: A review. *Marine*  
462        *Geology*, 361, 53-78. <https://doi.org/10.1016/j.margeo.2014.12.004>

463        Anthony, E.J., Impacted fluvial and coastal sediment connectivity in the Mediterranean: a brief review and  
464        implications in the context of global environmental change. In: Carboni, D., Matteucci, G., Bonora, L., De Vincenzi,  
465        M. (eds.), *Monitoring of Mediterranean Coastal Areas: problems and measurement techniques*. In press.

466        Anthony, E. J. & Aagaard, T. The lower shoreface: Morphodynamics and sediment connectivity with the upper  
467        shoreface and beach. *Earth-Science Rev.* DOI: <https://doi.org/10.1016/j.earscirev.2020.103334> (2020).

468        Anthony, E. J., Almar, R. & Aagaard, T. Recent shoreline changes in the Volta River delta, West Africa: the roles  
469        of natural processes and human impacts. *African Journal of Aquatic Science* 41, 81–87, DOI:  
470        10.2989/16085914.2015.1115751 (2016).

471        Anthony, E.J., Almar, R, Besset, M., Reyns, J., Laibi, R., Ranasinghe, R., Abessolo Ondo G., Vacchi, M. Response  
472        of the Bight of Benin (Gulf of Guinea, West Africa) coastline to anthropogenic and natural forcing, Part 2: Sources  
473        and patterns of sediment supply, sediment cells, and recent shoreline change. *Continental Shelf Research*, 173,  
474        93-103 (2019). <https://doi.org/10.1016/j.csr.2018.12.006>

475        Ardhuin, F. & Roland, A. Coastal wave reflection, directional spread, and seismoacoustic noise sources. *J.*  
476        *Geophys. Res. Ocean.* 117, DOI: <https://doi.org/10.1029/2011JC007832> (2012).



- 477 Bamunawala, J., Dastgheib, A., Ranasinghe, R., Van der Spek, A., Maskey, S., Murray, A. B., ... & Sirisena, T. A.  
478 J. G. (2020). A holistic modeling approach to project the evolution of inlet-interrupted coastlines over the 21st  
479 century. *Frontiers in Marine Science*, 7, 542.
- 480 Bamunawala, J., Ranasinghe, R. & Dastgheib, A. e. a. Twenty-first-century projections of shoreline change  
481 along inlet-interrupted coastlines. *Sci. Reports* DOI: <https://doi.org/10.1038/s41598-021-93221-9> (2021).
- 482 Barbier, E. B. (2011). *Capitalizing on nature: ecosystems as natural assets*. Cambridge University Press.
- 483 Benveniste, J. et al. Requirements for a coastal hazards observing system. *Front. Mar. Sci.* 6, 348, DOI: 10.3389  
484 /fmars.2019.00348 (2019).
- 485 Bergsma, E. W. & Almar, R. Coastal coverage of esa' sentinel 2 mission. *Adv. Space Res.* 65, 2636 – 2644, DOI:  
486 <https://doi.org/10.1016/j.asr.2020.03.001> (2020).
- 487 Besset, M., Anthony, E.J., Bouchette. Multi-decadal variations in delta shorelines and their relationship to river  
488 sediment supply: An assessment and review. *Earth-Science Reviews*, 193-199-219 (2019).  
489 <https://doi.org/10.1016/j.earscirev.2019.04.018>
- 490 Bruun, P. Sea level rise as cause of shore erosion. *J. Waterw. Harb. Div. ASCE* 88, 117–130 (1962).
- 491 Camenen, B., and M. Larson. A general formula for non-cohesive bed load sediment transport. *Estuarine,  
492 Coastal and Shelf Science* 63.1-2 (2005): 249-260.
- 493 Cao, A. et al. Future of Asian Deltaic Megacities under sea level rise and land subsidence: current adaptation  
494 pathways for Tokyo, Jakarta, Manila, and Ho Chi Minh City. *Curr. Opin. Environ. Sustain.* 50, 87–97, DOI: 10.1016  
495 /j.cosust.2021.02.010 (2021).
- 496 Cooper, J. et al. Sandy beaches can survive sea-level rise. *Nature Climate Change* DOI: 10.1038/s41558-020-  
497 00934-2 (2020).
- 498 da Silva, A. P. et al. Headland bypassing timescales: Processes and driving forces. *Sci. The Total. Environ.* 793,  
499 148591 , DOI: <https://doi.org/10.1016/j.scitotenv.2021.148591> (2021).
- 500 Dada, O., Almar, R., Morand, P. & Ménard, F. Towards West African coastal social-ecosystems sustainability :  
501 Interdisciplinary approaches. *Ocean and Coastal Management* (2021).
- 502 De Stefano, L., Petersen-Perlman, J.D., Sproles, E.A., Eynard, J., Wolf, A.T. Assessment of transboundary river  
503 basins for potential hydro-political tensions. *Global Environmental Change*, 45, 35-46 (2017),  
504 <https://doi.org/10.1016/j.gloenvcha.2017.04.008>.
- 505 Dean, R. Beach response to sea level change. *Ocean. Eng. Sci. v.9 of The Sea*, 869–887 (1990).



- 506 Dunn, F. E. et al. Projections of declining fluvial sediment delivery to major deltas worldwide in response to  
507 climate change and anthropogenic stress. *14*, 084034, DOI: 10.1088/1748-9326/ab304e (2019).
- 508 Everts, C. Sea level rise effects. *J. Waterw. Port, Coast. Ocean. Eng. Am. Soc. Civ. Eng.* 111 (6), 985–999 (1985).
- 509 Ezcurra, E. et al. A natural experiment reveals the impact of hydroelectric dams on the estuaries of tropical  
510 rivers. *Sci. Adv.* 5, eaau9875, DOI: 10.1126/sciadv.aau9875.
- 511 Farías, M. et al. Land-level changes produced by the mw 8.8 2010 Chilean earthquake. *Science* 2005, DOI:  
512 10.1126 / science.1192094 (2010).
- 513 Flaminio S., Piegay H., Le Lay Y.F. To dam or not to dam in an age of Anthropocene: Insights from a genealogy  
514 of media discourses. *Anthropocene*, 36, 100312 (2021). <https://doi.org/10.1016/j.ancene.2021.100312>
- 515 Flemming, B. W. (2011). 3.02-geology, morphology, and sedimentology of estuaries and coasts. *Treatise on*  
516 *Estuarine and Coastal Science*. Academic Press, Waltham, 7-38.
- 517 Gillet, H., Cirac, P. & Lagié, B. Pockmarks on the southern margin of the Capbreton canyon (south-eastern bay  
518 of Biscay). XI Int. Symp. on Oceanogr. Bay Biscay DOI: <https://doi.org/10.1038/s41598-020-77926-x> (2008).
- 519 Giosan, L. et al. Recent morphodynamics of the Indus delta shore and shelf. *Cont. Shelf Res.* 26, 1668–1684,  
520 DOI: <https://doi.org/10.1016/j.csr.2006.05.009> (2006).
- 521 Greve, P., Gudmundsson, L. & Seneviratne, S. Regional scaling of annual mean precipitation and water  
522 availability with global temperature change. *Earth Syst. Dyn.* 9, 227–240, DOI: [https://doi.org/10.5194/esd-9-](https://doi.org/10.5194/esd-9-227-2018)  
523 [227-2018](https://doi.org/10.5194/esd-9-227-2018) (2018).
- 524 Habel, M. e. a. Dam and reservoir removal projects: a mix of social-ecological trends and cost-cutting attitudes.  
525 *Sci. Reports* DOI: 10.1038/s41598-020-76158-3 (2020).
- 526 Hallermeier, R. J. Uses for a calculated limit depth to beach erosion. *Coast. Eng.* 1978 1493–1512, DOI: 10.1061  
527 / 9780872621909.090 (1978).
- 528 Hartmann, J. & Moosdorf, N. The new global lithological map database GLiM: A representation of rock  
529 properties at the Earth surface. *Geochem. Geophys. Geosystems* 13, DOI:  
530 <https://doi.org/10.1029/2012GC004370> (2012).
- 531 Hoegh-Guldberg, O. et al. Impacts of 1.5°C global warming on natural and human systems. IPCC Rep. (2018).
- 532 Huang, G. Time lag between reduction of sediment supply and coastal erosion. *Int. J. Sediment Res.* 26, 27–  
533 35, DOI:



- 534 Inman, D. L. & Brush, B. M. The Coastal Challenge: Fragile ribbons which border our land require more  
535 understanding, new technology, and resolute planning. *Science* 181, 20–32, DOI: 10.1126/science.181.4094.20  
536 (1973).
- 537 IPCC. Sea-level Rise (2021). [https://www.ipcc.ch/site/assets/uploads/2018/03/ipcc\\_far\\_wg\\_i\\_chapter\\_09.pdf](https://www.ipcc.ch/site/assets/uploads/2018/03/ipcc_far_wg_i_chapter_09.pdf)
- 538 Jeanson, M., Anthony, E.J., Charoux, S., Aubry, A., Dolique, F., 2021. Detecting the effects of rapid tectonically-  
539 induced sea-level rise on Mayotte Island since 2018 on beach and reef morphology, and implications for coastal  
540 vulnerability to marine flooding. *Geo-Mar. Lett.* 41, 51. [https://doi-org.insu.bib.cnrs.fr/10.1007/s00367-021-](https://doi-org.insu.bib.cnrs.fr/10.1007/s00367-021-00725-4)  
541 00725-4
- 542 Kamphuis. Alongshore sediment transport rate. *Coast. Oc. Engrg.* 117, 624–640 (1991).
- 543 Laugié, M., Michel, J., Pohl, A., Poli, E., & Borgomano, J. (2019). Global distribution of modern shallow-water  
544 marine carbonate factories: a spatial model based on environmental parameters. *Scientific reports*, 9(1), 1-14.
- 545 Leatherman, S. e. a. Sea level rise shown to drive coastal erosion. *Transactions Am. Geophys. Union* 81 (6),  
546 55–57 (2000).
- 547 Lehner, B. & G., G. Global river hydrography and network routing: baseline data and new approaches to study  
548 the world's large river systems. [www.hydrosheds.org](http://www.hydrosheds.org) (2013).
- 549 Lincke, D. & Hinkel, J. Coastal migration due to 21st century sea-level rise. *Earth's Futur.* 9, DOI:  
550 <https://doi.org/10.1029/2020EF001965> (2021).
- 551 Luijendijk, A. et al. The state of the world's beaches. *Sci. Reports* DOI: [https://doi.org/10.1038/s41598-018-](https://doi.org/10.1038/s41598-018-24630-6)  
552 24630-6 (2018).
- 553 Ly, C. K. The role of the Akosombo Dam on the Volta river in causing coastal erosion in central and eastern  
554 Ghana ( West Africa). *Mar. Geol.* 37, 323–332, DOI: 10.1016/0025-3227(80)90108-5 (1980).
- 555 Maffre, P., Ladant, J.-B., Moquet, J.-S., Carretier, S., Labat, D., Goddérès, Y., 2018. Mountain ranges, climate  
556 and weathering. Do orogens strengthen or weaken the silicate weathering carbon sink? *Earth Planet. Sci. Lett.*  
557 493, 174–185. <https://doi.org/10.1016/j.epsl.2018.04.034>.
- 558 Maneux, E., Probst, J. L., Veyssy, E. & Etcheber, H. Assessment of dam trapping efficiency from water residence  
559 time:
- 560 Marchesiello, P. et al. Erosion of the coastal mekong delta: Assessing natural against man induced processes.  
561 *Cont. Shelf Res.* DOI: <https://doi.org/10.1016/j.csr.2019.05.004> (2019).
- 562 Maul, G.A., Duedall, I.W.. Demography of Coastal Populations. In: Finkl, C.W., Makowski, C. (eds) *Encyclopedia*  
563 *of Coastal Science*. Encyclopedia of Earth Sciences Series. Springer, Cham (2019), [https://doi.org/10.1007/978-3-](https://doi.org/10.1007/978-3-319-93806-6_115)  
564 319-93806-6\_115



- 565 Mazières, A., Gillet, H., Castelle, B., Mulder, T., Guyot, C., Garlan, T., and Mallet, C., 2014, High-resolution  
566 morphobathymetric analysis and evolution of Capbreton submarine canyon head (Southeast Bay of Biscay—  
567 French Atlantic Coast) over the last decade using descriptive and numerical modeling: *Marine Geology*, v. 351, p.  
568 1–12, doi:10.1016/j.margeo.2014.03.001.
- 569 Melet, A. et al. Earth observations for monitoring marine coastal hazards and their drivers. *Surv. Geophys.*  
570 [Early access], p. [46 p.], DOI: 10.1007/s10712-020-09594-5 (2020).
- 571 Mentaschi, L., Voudoukas, M. & Pekel, J. e. a. Global long-term observations of coastal erosion and accretion.  
572 *Sci Rep* DOI: <https://doi.org/10.1038/s41598-018-30904-w> (2018).
- 573 Milliman, J. & Farnsworth, K. Runoff, erosion, and delivery to the coastal ocean. *River Disch. to Coast. Ocean.*  
574 *A Glob. Synth.* 43 (2011).
- 575 Milliman, J. & Ren, M. River flux to the sea: impact of human intervention on river systems and adjacent coastal  
576 areas. *Impact on coastal habitation* 57–83 (1995).
- 577 Milliman, J. D. & Farnsworth, K. L. *River Discharge to the Coastal Ocean: A Global Synthesis* (Cambridge  
578 University Press, Cambridge, 2011).
- 579 Morris, R., Boxshall, A. & Swearer, S. Climate-resilient coasts require diverse defence solutions. *Nat. Clim.*  
580 *Chang.* 485–487, DOI: <https://doi.org/10.1038/s41558-020-0798-9> (2020).
- 581 Morton, R. A., Miller, T. & Moore, L. Historical Shoreline Changes Along the US Gulf of Mexico: A Summary of  
582 Recent Shoreline Comparisons and Analyses. *J. Coast. Res.* 2005, 704 – 709, DOI: 10.2112/04-0230.1 (2005).
- 583 Mulder, J. P., Hommes, S. & Horstman, E. M. Implementation of coastal erosion management in the  
584 netherlands. *Ocean. & Coast. Manag.* 54, 888–897, DOI: <https://doi.org/10.1016/j.ocecoaman.2011.06.009>  
585 (2011). *Concepts and Science for Coastal Erosion Management ( Conscience )*.
- 586 Mulligan, M., van Soesbergen, A. & Saenz, L. GOODD, a global dataset of more than 38,000 georeferenced  
587 dams, DOI:
- 588 Nicholls, R. J. et al. A global analysis of subsidence, relative sea-level change and coastal flood exposure. *Nat.*  
589 *Clim. Chang.* 11, 338–342 (2021), DOI: <https://doi.org/10.1038/s41558-021-00993-z>.
- 590 Nienhuis, J. H., Ashton, A. D. & Giosan, L. What makes a delta wave-dominated? *Geology* 43, 511–514, (2015)
- 591 Nittrouer, J. A. & Viparelli, E. Sand as a stable and sustainable resource for nourishing the Mississippi River  
592 delta. *Nat. Geosci.* 7, 350–354, DOI: 10.1038/ngeo2142 (2014).
- 593 Noda, K. e. a. Debates over dam removal in japan : Debates over dam removal. *Water Environ. J.* DOI: 10.1111  
594 /wej. 12344 (2018).



- 595 Oppenheimer, M. et al. Sea level rise and implications for low-lying islands, coasts and communities. IPCC  
596 Special Rep. on Ocean. Cryosphere Chang. Clim. (2019).
- 597 Owens, P.N., 2020. Soil erosion and sediment dynamics in the Anthropocene: a review of human impacts  
598 during a period of rapid global environmental change. *Journal of Soils and Sediments*, 20, 4115-  
599 4143. <https://doi.org/10.1007/s11368-020-02815-9>
- 600 Passaro, M., Hemer, M. A., Quartly, G. D., Schwatke, C., Dettmering, D., & Seitz, F. (2021). Global coastal  
601 attenuation of wind-waves observed with radar altimetry. *Nature Communications*, 12(1), 1-13.
- 602 Pearson, S. G., van Prooijen, B. C., Elias, E. P. L., Vitousek, S. & Wang, Z. B. Sediment Connectivity: A Framework  
603 for Analyzing Coastal Sediment Transport Pathways. *J. Geophys. Res. Earth Surf.* 125, e2020JF005595, DOI:  
604 10.1029 / 2020JF005595 (2020).
- 605 Peduzzi, P. Sand, rarer than one thinks. *Environmental Development*, 11, 208-218 (2014),  
606 <https://doi.org/10.1016/j.envdev.2014.04.001>
- 607 Tran, Y. H., Marchesiello, P., Almar, R., Ho, D. T., Nguyen, T., Thuan, D. H., & Barthélemy, E. (2021). Combined  
608 longshore and cross-shore modeling for low-energy embayed sandy beaches. *Journal of Marine Science and  
609 Engineering*, 9(9), 979.
- 610 UNEP, 2019. Sand and Sustainability: Finding New Solutions for Environmental Governance of Global Sand  
611 Resources. <https://wedocs.unep.org/20.500.11822/28163>
- 612 Peucker-Ehrenbrink, B. Land2sea database of river drainage basin sizes, annual water discharges, and  
613 suspended sediment fluxes. *Geochem. Geophys. Geosystems* 10, DOI: 10.1029/2008GC002356 (2009).
- 614 Pilkey, O. H., & Cooper, J. A. G. (2014). Are natural beaches facing extinction?. *Journal of Coastal Research*, (70  
615 (10070)), 431-436.
- 616 Ranasinghe, R. On the need for a new generation of coastal change models for the 21st century. *Sci Rep* DOI:  
617 <https://doi.org/10.1038/s41598-020-58376-x> (2020).
- 618 Ranasinghe, R., Wu, C. S., Conallin, J., Duong, T. M., & Anthony, E. J. (2019). Disentangling the relative impacts  
619 of climate change and human activities on fluvial sediment supply to the coast by the world's large rivers: Pearl  
620 River Basin, China. *Scientific reports*, 9(1), 1-10.
- 621 Roelvink, D., Huisman, B., Elghandour, A., Ghonim, M., & Reyns, J. (2020). Efficient modeling of complex sandy  
622 coastal evolution at monthly to century time scales. *Frontiers in Marine Science*, 7, 535.
- 623 Vitousek, S., Barnard, P. L., Limber, P., Erikson, L., & Cole, B. (2017). A model integrating longshore and cross-  
624 shore processes for predicting long-term shoreline response to climate change. *Journal of Geophysical Research:  
625 Earth Surface*, 122(4), 782-806.



- 626 Restrepo, J., Kettner, A. & Syvitski, J. Recent deforestation causes rapid increase in river sediment load in the  
627 colombian andes. *Anthropocene* 13–28, DOI: <https://doi.org/10.1016/j.ancene.2015.09.001> (2015).
- 628 Rocle, N. et al. Paving the way to coastal adaptation pathways: An interdisciplinary approach based on  
629 territorial archetypes. *Environmental Science and Policy* 110, 34–45, DOI: 10.1016/j.envsci.2020.05.003 (2020).
- 630 Rosati, J., Dean, R. & Walton, T. The modified bruun rule extended for landward transport. *Mar. Geol.* 340,  
631 71–81, DOI: <https://doi.org/10.1016/j.margeo.2013.04.018> (2013).
- 632 Sharaf El Din, S. Longshore sand transport in the surf zone along the mediterranean egyptian coast. *Limnol.*  
633 *Oceanogr.* 19, 182–189 (1974).
- 634 Syvitski, J., Anthony, E.J., Saito, Y., Zăinescu, F., Day, J., Bhattacharya, J.P., Giosan, L.. Large deltas, small deltas:  
635 Towards a more rigorous understanding of coastal marine deltas. *Global & Planetary Change*, 2018, 103958  
636 (2022b). <https://doi.org/10.1016/j.gloplacha.2022.103958>
- 637 Syvitski, J.P.M., Kettner, A.J., Hannon, M.T., Hutton, E.W.H., Overeem, I., Brakenridge, G.R., Day, J.,  
638 Vörösmarty, C., Saito, Y., Giosan, L., Nicholls, R.J. Sinking deltas due to human activities. *Nature Geoscience* 2,  
639 681–689 (2009).
- 640 Syvitski, J. & Kettner, A. Sediment flux and the Anthropocene. *Philos. Transactions Royal Soc. A: Math. Phys.*  
641 *Eng. Sci.* 369, 957–975 (2011).
- 642 Syvitski, J. & Milliman, J. Geology, geography, and humans battle for dominance over the delivery of fluvial  
643 sediment to the coastal ocean. *J. Geol.* 115, DOI: 10.1086/509246 (2007).
- 644 Syvitski, J., Restrepo Angel, J., Saito, Y., Overeem, I., Vörösmarty, C., Wang, H., Olago, D.. Earth’s Sediment  
645 Budget during the Anthropocene. *Nature Reviews Earth & Environment* 3, 179–196 (2022a).  
646 <https://www.nature.com/articles/s43017-021-00253-w>
- 647 Syvitski, J. P. M. & Saito, Y. Morphodynamics of deltas under the influence of humans. *Glob. Planet. Chang.*  
648 57, 261–282 , DOI: 10.1016/j.gloplacha.2006.12.001 (2007).
- 649 Syvitski, J., Peckham, S., Hilberman, R. & Mulder, T. Predicting the terrestrial flux of sediment to the global  
650 ocean: a planetary perspective. *Sedimentary Geol.* 162, 5–24, DOI: 10.1016/S0037-0738(03)00232-X (2003).
- 651 Splinter, K. D., Turner, I. L., Davidson, M. A., Barnard, P., Castelle, B., & Oltman-Shay, J. (2014). A generalized  
652 equilibrium model for predicting daily to interannual shoreline response. *Journal of Geophysical Research: Earth*  
653 *Surface*, 119(9), 1936–1958.
- 654 Taherkhani, M. et al. Sea-level rise exponentially increases coastal flood frequency. *Sci. Reports* 10(6466)  
655 (2020).



- 656 Tay, C., Lindsey, E. O., Chin, S. T., McCaughey, J. W., Bekaert, D., Nguyen, M., ... & Hill, E. M. (2022). Sea-level  
657 rise from land subsidence in major coastal cities. *Nature Sustainability*, 1-9.
- 658 Tan, G. et al. Review and improvement of conventional models for reservoir sediment trapping efficiency.  
659 *Heliyon* 5, e02458, DOI: 10.1016/j.heliyon.2019.e02458 (2019).
- 660 Tiggeloven, T. et al. Global-scale benefit–cost analysis of coastal flood adaptation to different flood risk drivers  
661 using structural measures. *Nat. Hazards Earth Syst. Sci.* 20, 1025–1044, DOI: 10.5194/nhess-20-1025-2020 (2020).
- 662 Turner, R. E., Baustian, J. J., Swenson, E. M. & Spicer, J. S. Wetland Sedimentation from Hurricanes Katrina and  
663 Rita.
- 664 Valiente, N. G., Masselink, G., Scott, T., Conley, D. & McCarroll, R. J. Role of waves and tides on depth of closure  
665 and potential for headland bypassing. *Mar. Geol.* 407, 60–75, DOI:  
666 <https://doi.org/10.1016/j.margeo.2018.10.009> (2019).
- 667 Vitousek, S., Barnard, P. L. & Limber, P. Can beaches survive climate change? *J. Geophys. Res. Earth Surf.* 122,  
668 1060–1067, DOI: <https://doi.org/10.1002/2017JF004308> (2017).  
669 <https://agupubs.onlinelibrary.wiley.com/doi/pdf/10.1002/2017JF004308>.
- 670 Vousdoukas, M. I. et al. Sandy coastlines under threat of erosion. *Nat. Clim. Chang.* 10, 260–263, DOI:  
671 <https://doi.org/10.1038/s41558-020-0697-0> (2020).
- 672 Walling, D. & Webb, B. Erosion and sediment yield: a global overview. *IAHS Publ. Proc. Reports-Intern Assoc*  
673 *Hydrol. Sci.* 236, 3–20 (1996).
- 674 Warrick, J., East, A., & Dow, H. Fires, floods and other extreme events – How watershed processes under  
675 climate change will shape our coastlines. *Cambridge Prisms: Coastal Futures*, 1, E2 (2023). doi:10.1017/cft.2022.1
- 676 Warrick, J. A., Vos, K., East, A. E., & Vitousek, S. (2022). Fire (plus) flood (equals) beach: coastal response to an  
677 exceptional river sediment discharge event. *Scientific reports*, 12(1), 1-15.
- 678 Warrick, J. A. Littoral sediment from rivers: Patterns, rates and processes of river mouth morphodynamics.  
679 *Front. Earth Sci.* 8, 355, DOI: 10.3389/feart.2020.00355 (2020).
- 680 Warrick, J., Stevens, A., Miller, I.M., Harrison, S.R., Ritchie, A.C. & Gelfenbaum, G. World’s largest dam removal  
681 reverses coastal erosion. *Sci Rep* DOI: <https://doi.org/10.1038/s41598-019-50387-7> (2019).
- 682 Wessel, P. & Smith, W. H. F. A global self-consistent, hierarchical, high-resolution shoreline database. *J.*  
683 *Geophys. Res.* 101 (1996).
- 684 Wiegel, R. L. Nile delta erosion. *Sci. (New York, N.Y.)* 272, 337a, DOI: 10.1126/science.272.5260.337a (1996).



- 685 Willis, C. & Griggs, G. Reductions in Fluvial Sediment Discharge by Coastal Dams in California and Implications  
686 for Beach Sustainability. *The J. Geol.* 111, 167–182, DOI: 10.1086/345922 (2003).
- 687 Wright, L. D. & Nittrouer, C. A. Dispersal of river sediments in coastal seas: Six contrasting cases. *Estuaries* 18,  
688 494–508 (1995).
- 689 Xue, Z., Feng, A., Yin, P. & Xia, D. Coastal Erosion Induced by Human Activities: A Northwest Bohai Sea Case  
690 Study. *J. Coast. Res.* 2009, 723–733, DOI: 10.2112/07-0959.1 (2009).
- 691 Yang, H. F. et al. Different fates of the Yangtze and Mississippi deltaic wetlands under similar riverine sediment  
692 decline and sea-level rise. *Geomorphology* 381, 107646, DOI: 10.1016/j.geomorph.2021.107646 (2021).
- 693 Yang, H. F. et al. Human impacts on sediment in the Yangtze River: A review and new perspectives. *Glob.*  
694 *Planet. Chang.* 162, 8–17, DOI: 10.1016/j.gloplacha.2018.01.001 (2018).
- 695 Yang, S. L. et al. Role of delta-front erosion in sustaining salt marshes under sea-level rise and fluvial sediment  
696 decline. *Limnol. Oceanogr.* 65, 1990–2009, DOI: 10.1002/lno.11432 (2020).
- 697 Yang, S. L., Milliman, J. D., Li, P. & Xu, K. 50,000 dams later: Erosion of the Yangtze River and its delta. *Glob.*  
698 *Planet. Chang.* 75, 14–20, DOI: 10.1016/j.gloplacha.2010.09.006 (2011).
- 699 Yates, M. L., Guza, R. T., O'Reilly, W. C., Hansen, J. E., & Barnard, P. L. (2011). Equilibrium shoreline response  
700 of a high wave energy beach. *Journal of Geophysical Research: Oceans*, 116(C4).
- 701 Zăinescu, F., Anthony, E.J., Vespremeanu-Stroe, A., Besset, M., Tătui, F. Concerns about data linking delta land  
702 gain to human action. *Nature*, accepted.
- 703